http://dx.doi.org/10.5012/bkcs.2013.34.7.2029

Effects of Phosphorous-doping on Electrochemical Performance and Surface Chemistry of Soft Carbon Electrodes

Min-Jeong Kim, Jin-Tak Yeon,[†] Kijoo Hong,[‡] Sang-Ick Lee,[‡] Nam-Soon Choi,[†,*] and Sung-Soo Kim[*]

Graduate School of Green Energy Technology, Chungnam National University, Daejeon 305-764, Korea
[*]E-mail: kimss@cnu.ac.kr
[†]Interdisciplinary School of Green Energy, Ulsan National Institute of Science and Technology (UNIST), Ulsan 689-798, Korea. [*]E-mail: nschoi@unist.ac.kr
[‡]GS Energy, CRD Center, Daejeon 305-380, Korea
Received January 23, 2013, Accepted April 10, 2013

The impact of phosphorous (P)-doping on the electrochemical performance and surface chemistry of soft carbon is investigated by means of galvanostatic cycling and *ex situ* X-ray photoelectron spectroscopy (XPS). P-doping plays an important role in storing more Li ions and discernibly improves reversible capacity. However, the discharge capacity retention of P-doped soft carbon electrodes deteriorated at 60 °C compared to non-doped soft carbon. This poor capacity retention could be improved by vinylene carbonate (VC) participating in forming a protective interfacial chemistry on soft carbon. In addition, the effect of P-doping on exothermic thermal reactions of lithiated soft carbon with electrolyte solution is discussed on the basis of differential scanning calorimetry (DSC) results.

Key Words : Soft carbon, Phosphorous doping, Solid electrolyte interphase, Electrolyte, Thermal reactions

Introduction

Lithium-ion batteries (LIBs) have been the dominant energy storage technology for small-scale portable electronics.[1,2] Although LIBs have been successfully commercialized, a noticeable improvement in the energy density of LIBs is required to satisfy demand for high power and/or capacities for applications such as power tools and electric vehicles as well as for efficient use of renewable energies.[3] This can be attained by replacing the widely-used carbonaceous anodes and lithium cobalt oxide cathodes. It has been found that the structures of carbon materials substantially affect the stoichiometry of lithium in a carbon electrode.[4] It was recently reported that phosphorous (P) or boron (B)-doped disordered carbon exhibits improved reversible capacity.[5,6] The mechanism of Li storage in P-doped disordered carbon was investigated by ^{7}Li-NMR spectroscopy, providing meaningful information on the nature of the Li species in fully lithiated carbon.[6] From ^{7}Li-NMR studies, it was proposed that P-doping structurally provides greater storage of Li species and thereby reversible capacity is improved. To the best of our knowledge, however, the influence of the surface/interface chemistry on the electrochemical performance at elevated temperatures and thermal properties of P-doped soft carbon electrodes has not been reported.

Herein, we present the effects of P-doping on the charge and discharge cycling of soft carbon electrodes. In addition, the significant role of P-doping in the surface characteristics and thermal properties of soft carbon electrodes is discussed by means of X-ray photoelectron spectroscopy (XPS) compositional depth profiling and differential scanning calorimetry (DSC).

Experimental

Materials. The non-doped pristine soft carbon was prepared from a cokes precursor and P-doped soft carbon was made from a mixture of cokes and 4.5 wt % H_3PO_4 based on cokes. A homogenizer (SMT Co., Ltd. HF-93) was used to make the mixture homogeneous, and then the mixture was heated to 900 °C for 2 h in a nitrogen atmosphere. To evaluate the electrochemical properties of soft carbon electrodes, a slurry was prepared by mixing 90 wt % soft carbon as an active material with a 10 wt % poly(vinylidene fluoride) (PVDF) (KF1100, Kureha) binder dissolved in anhydrous *N*-methyl-2-pyrrolidinone (NMP, Aldrich). The resulting slurry was cast on a piece of copper foil (18 μm) and then dried in a vacuum oven at 110 °C for 1 h. The anode was next pressed to obtain proper electronic conductivity and its thickness without a copper current collector was around 18 μm. The electrolyte used for electrochemical tests of soft carbon electrodes was 1 M lithium hexafluorophosphate ($LiPF_6$) dissolved in a mixture of ethylene carbonate (EC)/ethylmethyl carbonate (EMC) (30/70, v/v) (Soulbrain Co. Ltd.). 1 wt % vinylene carbonate (VC, Soulbrain Co. Ltd.) was used as an additive to form an effective solid electrolyte interphase (SEI) layer on the soft carbon electrode.

Measurements. The surface morphology of the soft carbon electrodes was observed by means of a field emission scanning electron microscope (FE-SEM; JSM-7000F). The cross-sectional morphology of the soft carbon was obtained using a focused ion beam (Quanta 3D FEG) with a Ga source. During the acquisition of the images, an energy dispersive spectrometer (EDS) was also used to determine the chemical components in the region under investigation. X-ray diffrac-

tion (XRD) patterns of soft carbon electrodes with and without phosphorous (P)-doping were recorded using monochromatic Cu-Kα radiation. X-ray photoelectron spectroscopy (XPS) analyses for soft carbon anodes rinsed in dimethyl carbonate (DMC, water content: 13 ppm) were carried out with a MultiLab 2000 spectrometer using focused monochromatized Al Kα radiation (hν = 1486.6 eV). The analyzed area of each sample was 600 μm and the pressure in the analysis chamber was 5×10^{-10} mbar. The approximate rate for XPS depth analyses was 1 nm min^{-1}. To measure the thermal properties of lithiated soft carbon electrodes with electrolytes, coin-type half cells were charged to 0.01 V *vs*. Li/Li^+ and then carefully opened in a dry room. The retrieved electrodes were rinsed in a DMC solvent to remove residual electrolyte and then dried. The resulting lithiated soft carbon electrode was sealed together with an electrolyte in a hermetic stainless-steel pan (Perkin Elmer). All of the differential scanning calorimetry (DSC, DuPont TA Instrument 2000) measurements were carried out at a heating rate of 5 °C min^{-1} over a range of 40-350 °C. The amount of entrapped electrolyte was 30 wt % based on the lithiated soft carbon.

Electrochemical Measurements. A coin-type half cell (2016) with a soft carbon anode and a Li metal electrode was assembled in an argon filled glove box with less than 1 ppm of both oxygen and moisture. Microporous polyethylene film (Celgard 2400) was used as a separator. Precycling for soft carbon/Li cells were galvanostatically performed at a rate of C/5 using a computer-controlled battery measurement system (WonATech WBCS 3000). Galvanostatic discharge

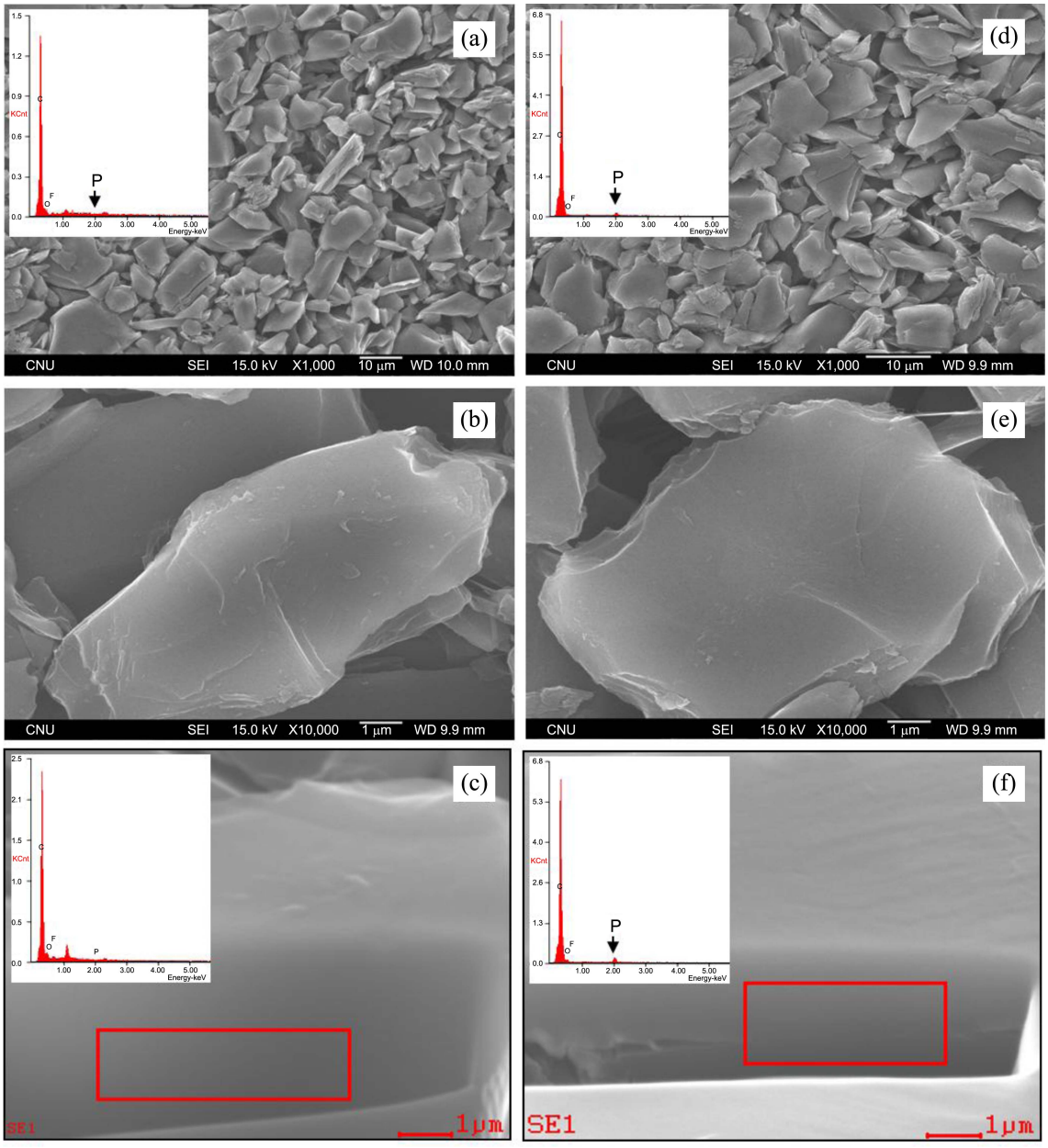

Figure 1. SEM images and EDS spectra for (a) and (b) non-doped soft carbon electrode surface, (c) the cross section of non-doped soft carbon particle, (d) and (e) P-doped soft carbon electrode surface, (f) the cross section of P-doped soft carbon particle.

and charge cycling of soft carbon/Li cells was carried out in a potential window from 0.01 to 2.5 V *versus* Li/Li^+ at a rate of C/5.

Results and Discussion

Figure 1 shows SEM images and EDS spectra of soft carbon particles with and without phosphorous (P)-doping. Soft carbon particles with and without P-doping have analogous surface morphology, as presented in Figures 1(a) and (d). P-doped soft carbon showed an intense signal related to P and the calculated P content was 4.37%, as shown in the EDS spectrum of Figure 1(d). The SEM image and EDS spectrum of Figure 1(f) provide evidence that the P-doped soft carbon has P atoms in its bulk phase.

The XRD patterns of soft carbon with and without P-

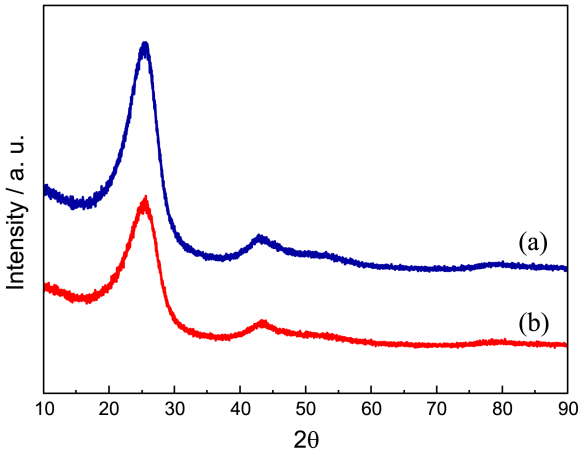

Figure 2. XRD patterns of soft carbon electrodes (a) without P-doping, (b) with P-doping.

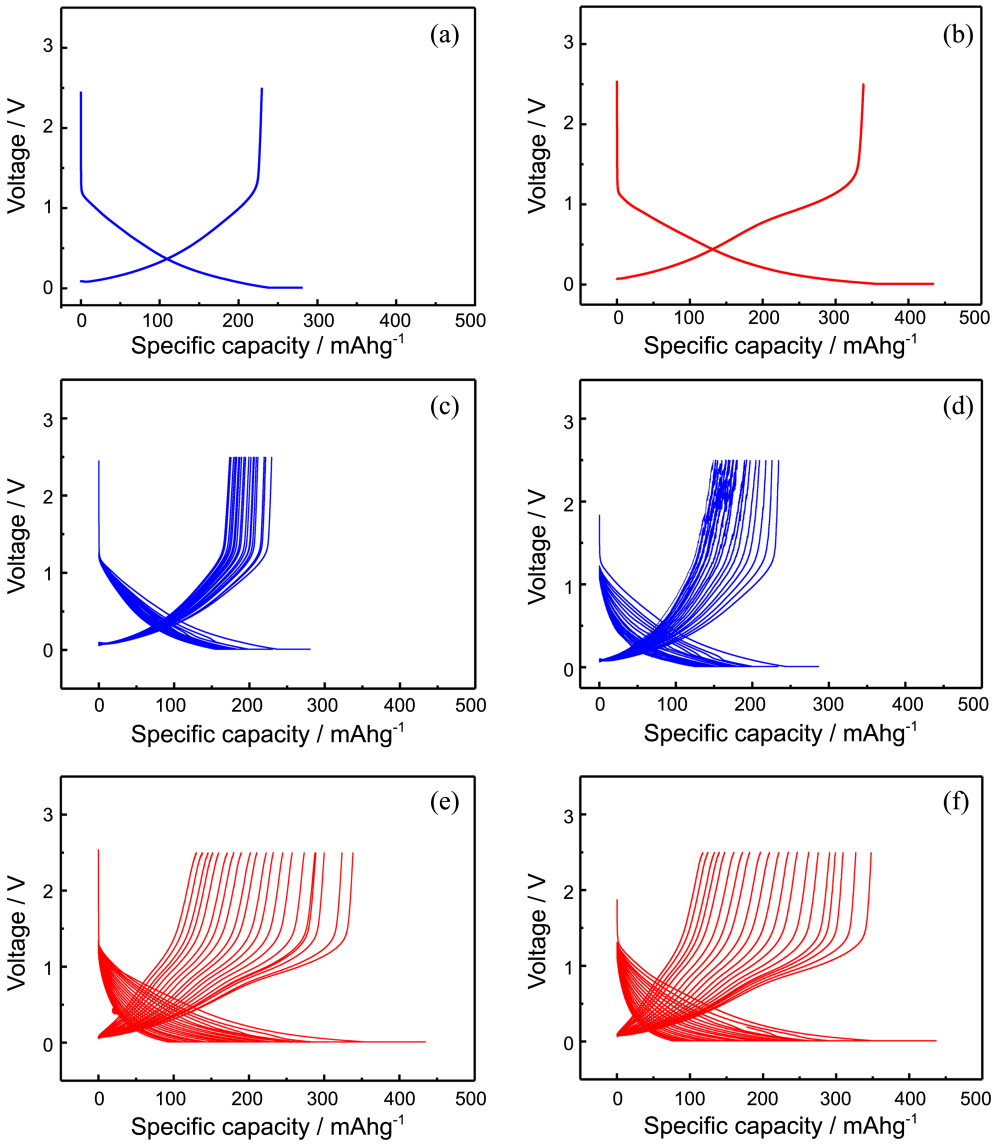

Figure 3. Charge and discharge curves of soft carbon electrodes (a) without P-doping, (b) with P-doping between 0.01 and 2.5 V *versus* Li/Li^+ at a rate of 0.2C during precycling, cycling performance of soft carbon electrodes (c) without P-doping at room temperature (d) without P-doping at 60 °C, (e) with P-doping at room temperature, (f) with P-doping at 60 °C.

doping are shown in Figure 2. There are two broad diffraction peaks around 2θ = 25.3 and 43° in each spectrum, corresponding to the diffraction of (002) and (100), respectively.[7-9] Importantly, it is found that the d spacing is slightly increased from 3.5019 to 3.5122 by P-doping. This increased distance between the graphene layers in the crystallized region may be due to the interaction between P and the neighboring graphitic layers.

Figures 3(a) and (b) display the charge and discharge curves of soft carbon-based electrodes at the first cycle. Soft carbon-based electrodes have no obvious potential plateaus, because there are various kinds of Li reaction sites.[10] Li can intercalate into the graphene layers of small crystallites and also react with the carbon atoms at the edge of the graphitic layers. Moreover, Li can locate on the surface of crystallites

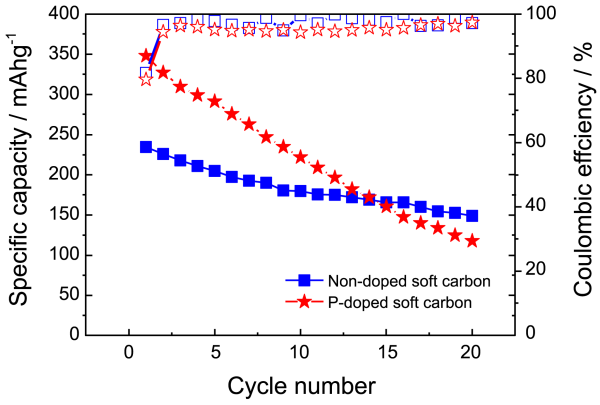

Figure 4. Discharge capacity retention (filled symbol) and coulombic efficiency (empty symbol) of the soft carbon electrodes during 20 cycles at 60 °C.

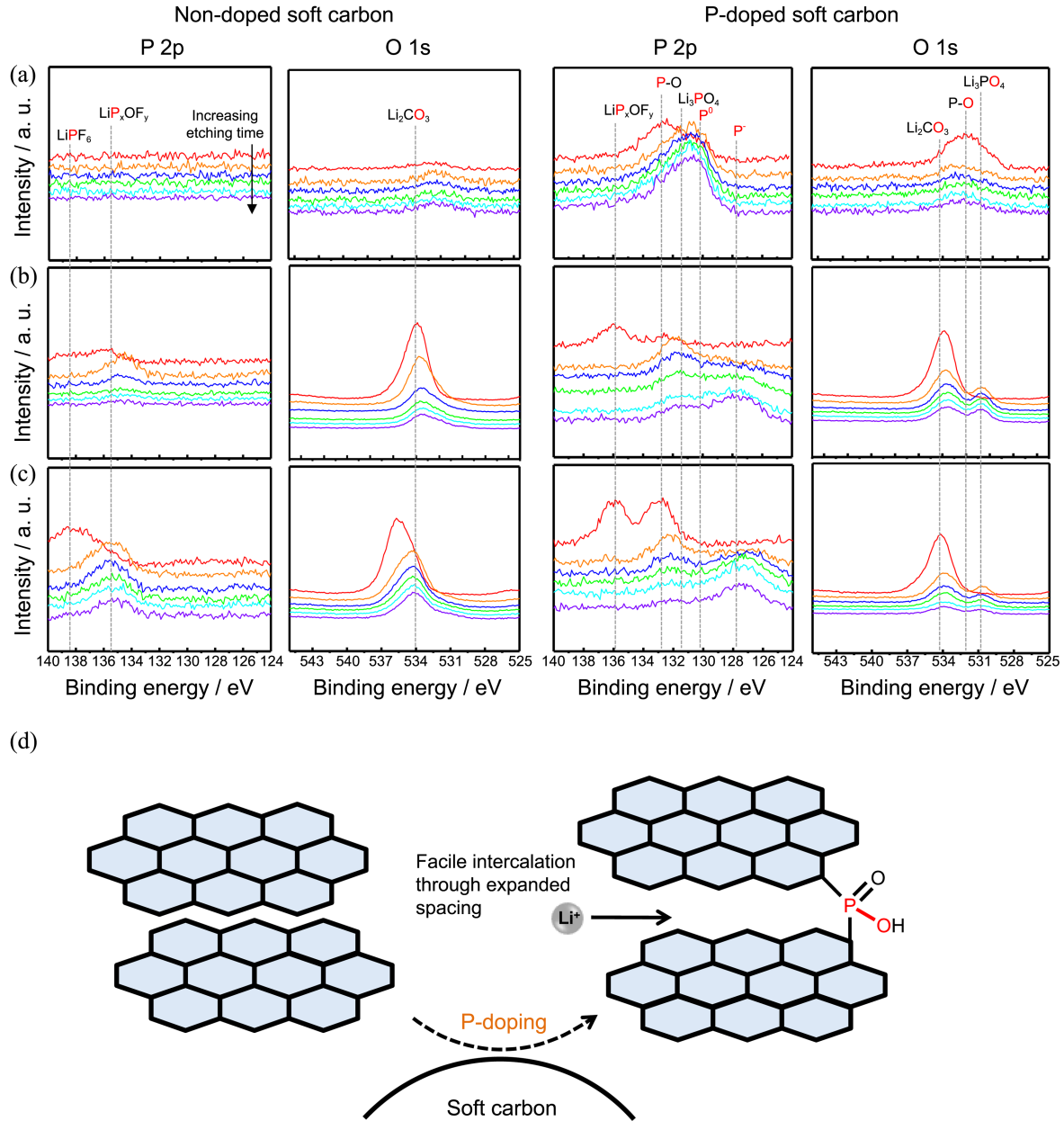

Figure 5. P 2p and O 1s XPS spectra for non-doped soft carbon and P-doped soft carbon (a) before cycle, (b) after 20 cycles at room temperature, (c) after 20 cycles at 60 °C.

by interaction with carbon atoms on the surface of the graphitic layer. Importantly, higher charge and discharge capacities are obtained for the P-doped soft carbon. It has been reported that the improved reversible capacity of soft carbon with P-doping is likely due to the increase of sites accepting Li ions and increased interlayer spacing allowing facile Li intercalation, as depicted in Figure 5(d).[12,13] In addition to this reaction mechanism, P species may make crosslinking structures between crystallites at the edge-plane of graphene layers and thereby P-doped soft carbon can store more Li ions compared to non-doped soft carbon.[6,11] The initial coulombic efficiencies of P-doped and non-doped soft carbon was 81.6 and 77.7%, respectively. This implies that P-doping provokes the irreversible interfacial reaction during initial lithiation. Furthermore, the XRD results of P-doped and non-doped soft carbon showed no remarkable changes in d(002) spacing. With the decreased initial efficiency and no measurable changes in d(002) spacing by P-doping, it is reasonable to consider the major role of P-doping is surface effect in our samples. Charge and discharge curves of soft carbon with and without P-doping at room temperature and 60 °C during 20 cycles are shown in Figures 3(c)-(f). It is found that the discharge capacity of the P-doped soft carbon-based electrode was considerably decreased and was lower than that of soft carbon without P doping after 15 cycles, as shown in Figures 3 and 4. As clearly seen in Figure 4, the discharge capacity retention and coulombic efficiency of P-doped soft carbon were relatively inferior compared to non-doped soft carbon at 60 °C. It is thought that the continuous Li consumption by electrolyte decomposition takes place and the resulting surface layer hinders the electrochemical reversibility of P-doped soft carbon at 60 °C. In order to investigate the effect of P-doping on the surface chemistry of soft carbon, the XPS spectra for P 2p, O 1s, C 1s, and F 1s were obtained from soft carbon electrodes before and after 20 cycles at room temperature and 60 °C. The spectra are shown in Figures 5-7 and peak assignments are summarized in Table 1.[14] Figure 5 shows the P 2p and O 1s spectra for soft carbon electrodes with and without P-doping; as expected, P-O (C-P-O) species indicated by the P 2p peak at 132.5 eV and the O 1s peak at 532 eV are observed for the pristine soft carbon with P-doping, as shown in Figure 5(a). The P-O species may be formed by P-doping, as illustrated in Figure 5(d). This results is in good agreement with the previous reports[15,16] The lower binding energy peak at 128 eV assigned to reduced phosphorus (denoted as P^-) was observed on the inner layer of the P-doped soft carbon after 20 cycles and was more intense after cycling at 60 °C. This reduced phosphorus (P^-) may be combined with the Li^+ ions and result in the formation of Li–P alloy compound.[17] The outer surface layer of P-doped soft carbon shows two peaks at 136 and 132.5 eV arising from Li_xPOF_y and P-O species after 20 cycles at room temperature, respectively. These peaks became more intense after 20 cycles at 60 °C, as shown in Figure 5(c). The P-O species produced by P-doping may participate in the electrolyte decomposition at the soft carbon surface. In addition, the P-doped soft carbon cycled at room temperature and 60 °C showed a pronounced peak attributed to Li_3PO_4 at around 132 eV. Li_3PO_4 may be formed by the reaction of Li ions with the P-O species. In comparison, a very weak peak corresponding to Li_xPOF_y appeared at 136 eV for the soft carbon electrode without P doping after 20 cycles at room temperature. After cycling at 60 °C, a more intense peak attributed to P-O from Li_xPOF_y was clearly observed for the inner layer of non-doped soft carbon and a peak corresponding to $LiPF_6$ at 138 eV appeared at the outer layer of non-doped soft carbon, as seen in Figure 5(c). A peak related to the P-O species generated by P-doping at 531 eV is clearly shown for the P-doped soft carbon before cycling, as presented in the O 1s spectra of Figure 5(a). The XPS results clearly showed that H_3PO_4 used for P doping forms phosphate species on the soft carbon electrode, as depicted in the P 2p and O 1s spectra of Figure 5(a). The resulting phosphate species may lead to significant decomposition of $LiPF_6$ salt during cycling. A peak corresponding to Li_2CO_3 formed by EC reduction appeared at 534 eV for both soft carbon electrodes after cycling at room temperature and 60 °C. Importantly, a more intense Li_2CO_3 peak was observed on the non-doped soft carbon compared with P-doped soft carbon even after depth profiling. This means that the surface layer formed on the non-doped soft carbon mainly consists of Li_2CO_3, as depicted in Figure 8.

Table 1. XPS data of the surface species formed on the soft carbon electrodes[14]

	Binding energy (eV)			
	P 2p	O 1s	C 1s	F 1s
Reduced phosphorous (P^-)	128			
P element (P^0)	130			
Li_3PO_4	131			
Li_xPOF_y, Li_xPF_y	136			690
P-O species	132.5-134	531		
$LiPF_6$	138			
$ROCO_2Li$		533	289	
Li_2CO_3		534	291	
C (sp^2, sp^3)			284.5	
PVDF			291.5	688
LiF				686.5-687

Figure 6 shows the C 1s spectra for soft carbon electrodes with and without P doping. It should be noted that phosphorus compounds cannot be clearly determined from C 1s region because binding energy of C-P-O bonding is similar to binding energy in alcohol and ether groups (C-O-C).[18] A peak corresponding to the $–CO_2$-group of lithium alkyl carbonate ($R-OCO_2Li$) appeared at 289 eV on both soft carbon electrodes cycled at room temperature, as displayed in Figure 6(b). The P-doped soft carbon cycled at 60 °C showed the $R-OCO_2Li$ peak at around 289 eV and there was no peak arising from lithium alkyl carbonate after depth profiling. On the other hand, a Li_2CO_3 peak at 291 eV appeared on non-doped soft carbon cycled at 60 °C along with R-

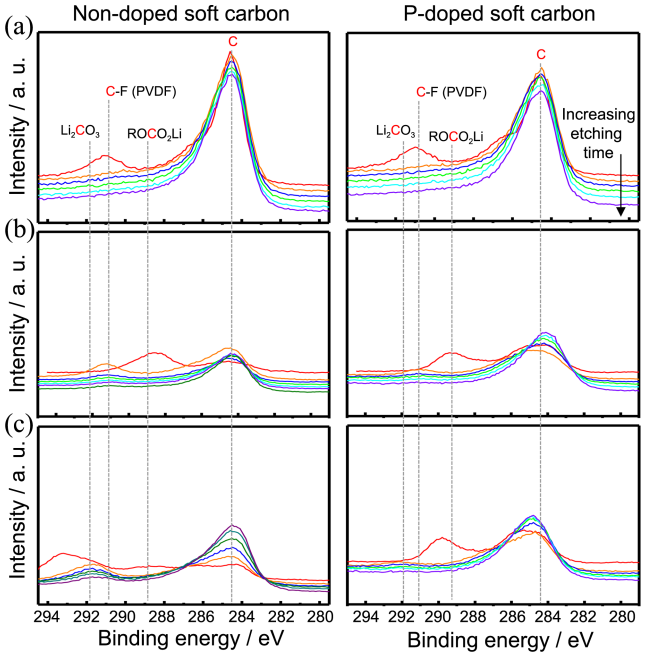

Figure 6. C 1s XPS spectra for non-doped soft carbon and P-doped soft carbon (a) before cycle, (b) after 20 cycles at room temperature, (c) after 20 cycles at 60 °C.

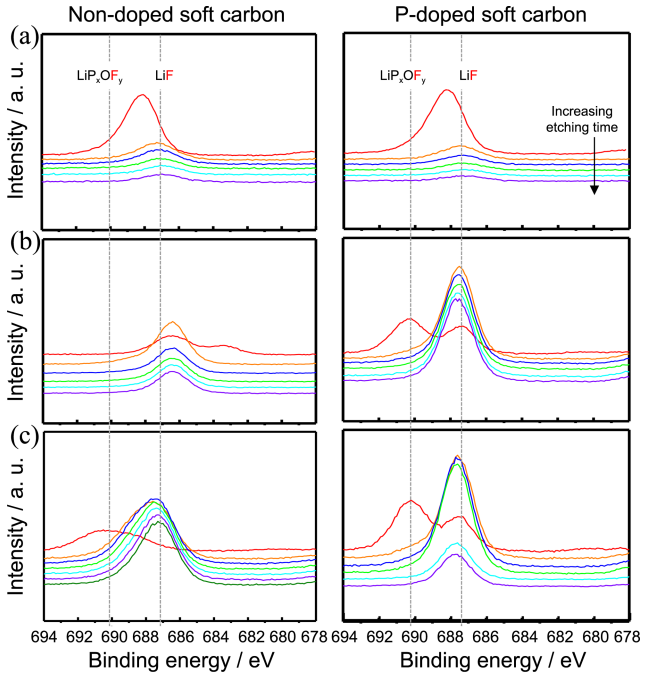

Figure 7. F 1s XPS spectra for non-doped soft carbon and P-doped soft carbon (a) before cycle, (b) after 20 cycles at room temperature, (c) after 20 cycles at 60 °C.

OCO_2Li at the outer layer and was still observed in the inner layer after depth profiling, as shown in Figure 6(c). The F 1s XPS spectra of soft carbon electrodes before and after cycling are shown in Figure 7. A C-F peak originating from a PVdF binder at 688 eV was detected on both soft carbon electrodes before cycling. The peak intensity corresponding to LiF at around 687 eV on the P-doped soft carbon was

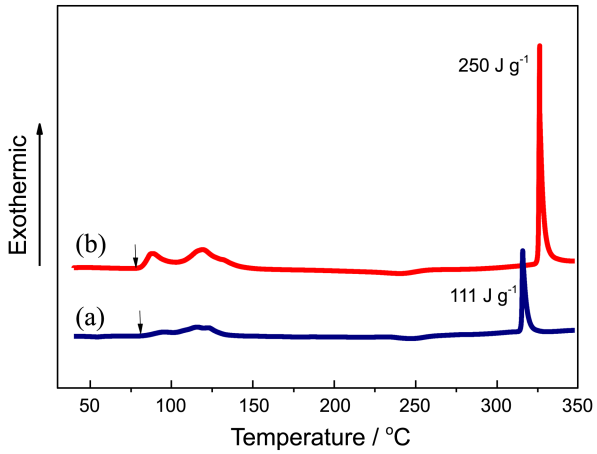

Figure 8. DSC thermograms of (a) non-doped soft electrode with an electrolyte, (b) P-doped soft carbon electrode with an electrolyte.

much higher than that of non-doped soft carbon, as shown in Figures 7(b) and (c). This result suggests that the P-O species formed by P-doping accelerate the $LiPF_6$ salt decomposition during cycling at 60 °C and result in capacity fading due to the depletion of salt along with solvent.

To understand the thermal properties of fully lithiated soft carbon with and without P-doping in the presence of an electrolyte solution, differential scanning calorimetry (DSC) experiments were conducted. Figure 8 presents the DSC heating curves of soft carbon electrodes with and without P-doping after being fully charged to 0.01 V *vs.* Li/Li^+. The lithiated soft carbon electrode without P-doping showed the onset of the first exothermic peak at 85 °C, associated with thermal decomposition reactions between the SEI layer and an electrolyte solution, as seen in Figure 8(a).[9] On the other hand, for lithiated P-doped soft carbon, the onset temperature related to thermal decomposition of SEI with an electrolyte was slightly lowered to 80 °C, as shown in Figure 8(b). This is in good agreement with poor capacity retention of P-doped soft carbon electrodes at elevated temperatures. It is clear that P-doping in soft carbon produces a thermally unstable SEI layer. The prominent exothermic peak at 312 °C for non-doped soft carbon is attributed to the exothermic decomposition reactions of the lithiated soft carbon electrode with volatile organic solvents, which result in a large heat evolution.[19,20] According to Yamaki *et al.*,[20] the thermal reactions of lithiated graphite particles covered with a PVdF binder with an electrolyte begin at around 300 °C, because the protective effect of the PVdF binder is not sufficient at elevated temperatures. From this point of view, it is thought that the newly exposed lithiated soft carbon by swelling of the PVdF binder at elevated temperatures thermally decomposes in the presence of an electrolyte and generates a large amount of exothermic heat at temperature over 300 °C, as shown in Figure 8. Importantly, the P-doping considerably increased the intensity of the exothermic peaks near 325 °C, as shown in Figure 8(b). It is clear that that P-doping cannot ensure thermal stability of soft carbon under harsh conditions.

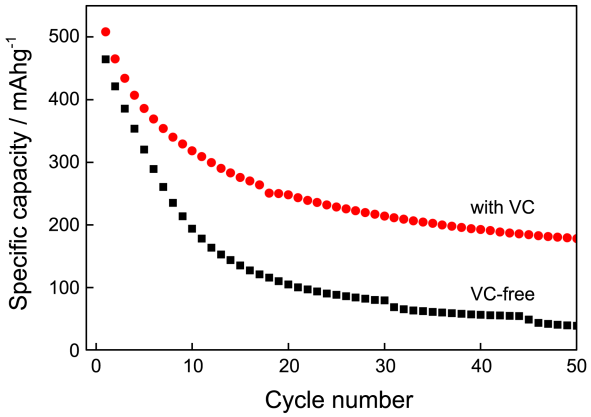

Figure 9. Discharge capacity retention of P-doped soft carbon electrodes with and without a VC additive during 50 cycles at 60 °C.

In order to alleviate the negative impact of the P-O species on the surface chemistry of P-doped soft carbon, vinylene carbonate (VC), which has been widely used as an additive for forming a stable solid electrolyte interphase (SEI), was introduced.[21-26] Indeed, the discharge capacity retention of P-doped soft carbon was drastically improved at 60 °C, as shown in Figure 9. This is likely because VC modified the soft carbon electrode/electrolyte interface and suppressed the reductive decomposition of the P-O species formed on the soft carbon electrode by P-doping.

Conclusions

The effects of P-doping on the galvanostatic cycling of soft carbon electrodes were described. P-doped soft carbon showed poor capacity retention at room temperature and 60°C due to the formation of an unstable surface film. XPS depth profiling analyses confirmed that the surface layer formed on the P-doped soft carbon is mostly composed of inorganic species such as LiF and salt decomposition products rather than lithium alkyl carbonates, in contrast with non-doped soft carbon, where lithium alkyl carbonates are the dominant species. DSC results indicated that P-doping triggers exothermic thermal reactions between lithiated soft carbon and the electrolyte solution at lower temperature and generates large exothermic heat at elevated temperatures.

Acknowledgments. The authors gratefully acknowledge for financial support by IT R&D program of MKE/KEIT (K10039155, Soft carbon anode material development for high capacity rechargeable battery). Also, this work was partly supported by the National Research Foundation of Korea Grant funded by the Korean Government (MEST) (NRF-2011-C1AAA001-0030538).

References

1. Tarascon, J. M.; Armand, M. *Nature* **2001**, *414*, 359.
2. Cheng, F.; Liang, J.; Tao, Z.; Chen, J. *Adv. Mater.* **2011**, *23*, 1695.
3. Choi, N.-S.; Yao, Y.; Cui, Y.; Cho, J. *J. Mater. Chem.* **2011**, *21*, 9825.
4. Matsumura, Y.; Wang, S.; Mondori, J. *Carbon* **1995**, *33*, 1457.
5. Komaru, A.; Azuma, H.; Nishi, Y. Japan patent, No. H5-74457.
6. Wang, S.; Matsui, H.; Matsumira, Y. *Synthetic Metals* **1999**, *103*, 2521.
7. Zheng, T.; Liu, Y.; Fuller, E. W.; Tseng, S.; von Sacken, U.; Dahn, J. R. *J. Electrochem. Soc.* **1995**, *142*, 2581.
8. Dahn, J. R.; Sleigh, A. K.; Reimers, J. N.; Zhong, Q.; Way, B. M. *Electrochim. Acta* **1993**, *38*, 1179.
9. Gong, J.; Wu, H.; Yang, Q. *Carbon* **1999**, *37*, 1409.
10. Wang, S.; Matsumura, Y.; Maeda, T. *Synthetic Metals* **1995**, *71*, 1759.
11. Tran, T. D.; Feikert, J. H.; Song, X.; Kinosita, K. *J. Electrochem. Soc.* **1995**, *142*, 3297.
12. Wu, Y.; Rahm, E.; Holze, R. *Electrochim. Acta* **2002**, *47*, 3491.
13. Wu, Y.; Fang, S.; Jiang, Y. *J. Power Sources* **1998**, *75*, 201.
14. Verma, P.; Maire, P.; Novák, P. *Electrochimica Acta* **2010**, *55*, 6332.
15. Laine, J.; Calafat, A.; Labady, M. *Carbon* **1989**, *27*, 191.
16. Oh, S.; Rodriquez, N. *J. Mater. Res.* **1993**, *8*, 2879.
17. Zhang, H.; Lu, Y.; Gu, C.-D.; Wang, X.-L.; Tu, J.-P. *Cryst. Eng. Comm.* **2012**, *14*, 7942.
18. Puziy, A. M.; Poddubnaya, O. I.; Socha, R. P.; Gurgul, J.; Wisniewski, M. *Carbon* **2008**, *46*, 2113.
19. Choi, N.-S.; Profatilova, I. A.; Kim, S.-S.; Song, E. H. *Thermochim. Acta* **2008**, *480*, 10.
20. Yamaki, J. I.; Takatsuji, H.; Kawamura, T.; Egashira, M. *Solid State Ionics* **2002**, *148*, 241.
21. Jeong, S.-K.; Inaba, M.; Mogi, R.; Iriyama, Y.; Abe, T.; Ogumi, Z. *Langmuir* **2001**, *17*, 8281.
22. Aurbach, D.; Gamolsky, K.; Markovsky, B.; Gofer, Y.; Schmidt, M.; Heider, U. *Electrochim. Acta* **2002**, *47*, 1423.
23. Buqa, H.; Wursig, A.; Vetter, J.; Spahr, M. E.; Krumeich, F.; Novak, P. *J. Power Sources* **2006**, *153*, 385.
24. Ota, H.; Shima, K.; Ue, M.; Yamaki, J.-I. *Electrochim. Acta* **2004**, *49*, 565.
25. Zhang, S. S.; Xu, K.; Jow, T. R. *Electrochim. Acta* **2006**, *51*, 1636.
26. Herstedt, M.; Rensmo, H.; Siegbahn, H.; Edström, K. *Electrochim. Acta* **2004**, *49*, 2351.